Letter

Observation of Double-strangeness Nuclei using Nuclear-emulsion Technology

Aung Nay Lin Nyaw[1][*], Hiroyuki EKAWA[2], Manami FUJITA[3], Shuhei HAYAKAWA[3], Ayumi KASAGI[1,2], Phyo Myat Lin[1], Kazuma NAKAZAWA[1,4], Junya YOSHIDA[2,5], Masahiro YOSHIMOTO[4]

Abstract: The J-PARC E07 experiment aimed to systematically detect double-strangeness nuclei with emulsion technologies. Thirty-three events were detected within 2 years by following of Ξ^- tracks. One event of D001 among them was examined to identify the production and decay processes by energy and momentum conservation obtained from the track lengths and emission angles of daughter particles. The event was determined to be $^{10}_{\Lambda\Lambda}$Be (^{8}Be and two Λ particles) as the most likely case assuming Ξ^- capture in the atomic $3D$ state of ^{14}N. The binding energy of the two Λ hyperons and the core nucleus of this double-Λ hypernucleus was 15.22 ± 2.78 MeV, and the Λ-Λ interaction strength was 1.80 ± 2.78 MeV.

Key words: Double hypernuclei, Double strangeness, Binding energy, J-PARC E07, Nuclear emulsion

Double hypernuclei (DH) with two units of strangeness (S) -such as double-Λ hypernuclei (DLH) or Ξ hypernuclei-have been studied experimentally with Λ and Ξ hyperons having one and two units of S, respectively for more than 50 years [1-9]. In the case of DLH, we can analyze the binding energy ($B_{\Lambda\Lambda}$) between two Λ hyperons and the core nucleus, as well as the interaction strength ($\Delta B_{\Lambda\Lambda}$) of the two Λ hyperons with each other. The $B_{\Lambda\Lambda}$ and $\Delta B_{\Lambda\Lambda}$ gives us an information about Λ-Λ and Ξ-N (nucleon) interactions, and $\Lambda\Lambda$ - ΞN mixing effect. This information is important for understanding not only specific issues in nuclear physics but also the formation of neutron stars. To measure $B_{\Lambda\Lambda}$ and $\Delta B_{\Lambda\Lambda}$ is equal to measure the mass of DH, whose mass energy can be obtained from the track ranges of daughter nuclei by the decay of DH. Nuclear emulsion is the best way to analyse DH, as it can detect very rare, low-energy, or short-lived particles with sub-µm spatial resolution. This article introduces nuclear-emulsion technology and the nuclide identification method of DH events analysed by using an optical microscope with an example of D001 event.

In the previous experiment of KEK E373 (E373), we detected 9 DH [10]. Among these, a double-Λ hypernuclear event named NAGARA was the first case uniquely identified as $^{6}_{\Lambda\Lambda}$He [3)5)]. From the NAGARA event, $\Delta B_{\Lambda\Lambda}$ was measured to be 0.67 ± 0.17 MeV, which means Λ-Λ interaction is weakly attractive. In order to know the Λ-Λ interaction depending on the differences of core nuclei, several DLH events were necessary to be identified uniquely. The most recent experiment of J-PARC E07 (E07), which aimed at detecting about 100 DH events using approximately 10 times as much data as

E373. One event in the 14 DLH events, named MINO [8], was likely interpreted as $^{11}_{\Lambda\Lambda}$Be with $\Delta B_{\Lambda\Lambda}$ of 1.87 ± 0.37 MeV, which is not consistent with that of the NAGARA event. The other DLH events are now under analysis.

The experimental process at both experiments includes 1) emulsion sheet making, 2) beam exposure, 3) photographic development and 4) detection and analyses of DH, and that of E07 is as follows. We produced dedicated photographic-emulsion sheets from nuclear emulsion gel for the use of this E07 experiment. We prepared 2.1 tonnes of the emulsion gel (Fuji: NU-3GIFL), which was three times as much as the amount used in E373. The gel of 2,930 g is melted in a hot water bath of 40 °C with plasticizer of 164 mL (181 g). The melted emulsion was poured into an area of 71 × 70 cm² framed by acrylic square bars on a polystyrene (PS) film support of 40 µm-thick, which was spread on an acrylic plate on a level block made of stone. Since the fringe of the emulsion gel undergoes heavy distortion in the drying process, dummy gel made of gelatin and plasticizer was applied around the layer of emulsion gel in a 76 × 76 cm² region after the emulsion gel was set with cool air (20 °C) from an air conditioner. The gel layers on the acrylic plate were installed in the drying cabinet, and dried at 30 °C and 75% relative humidity (R.H.) for 2 days, then we got 450 µm-thick emulsion sheets (thick sheet). On the third day after coating, we coated the surface of emulsion layer with 0.3% gelatin solution to prevent the precipitation of silver on a photographic development process. On the fourth day, we repeated the above processes on the backside of the sheet and finally dried at 25 °C and 60% R.H. for one day. The

large dried sheet with a thickness of nearly 1 mm was cut into 35.0 × 34.5 cm². One manufacturing cycle produced 144 emulsion sheets of this size. A thin sheet of a PS film of 180 μm-thick with 100 μm-thick emulsion layers on either side was produced in the same way as described above. Both sheets have a thickness accuracy of 5%. The numbers of prepared thick and thin sheets were 1,298 and 236, respectively.

To avoid the recording of tracks in the sheet from cosmic radiation, all the sheets were kept in an underground laboratory of Kamioka Observatory (University of Tokyo) before the beam exposure. Because our beam times were postponed to 3 years (20% emulsion) and 4 years (80% emulsion) after the production of sheets, the sheets were stored in a box of 40 × 40 × 150 cm³ dimensions at 17 ± 1 °C shielded by lead blocks of 10 cm thick to prevent Compton electrons scattered by γ-rays in the Kamioka mine. By keeping the sheets in Kamioka for 3 years, the record of cosmic ray and Compton electron were respectively suppressed to 6.5% and 20% from the ones kept in a refrigerator of Gifu University for 2 years. Moreover, we conducted the forced fading [11] just before beam exposure to erase the recorded latent images by keeping all the sheets for 100 h at 25 °C and 90% R.H.

Figure 1 presents the setup for the beam exposure of E07. We irradiated the diamond target with $1.13×10^{11}$ K⁻ particles of momentum 1.8 GeV/c to produce Ξ⁻ particles for DH measurement. In the K⁻ reaction with a proton (p), we tagged K⁺ as a signal for Ξ⁻ production with a magnet spectrometer (KURAMA), in which the reaction of K⁻+ p → K⁺+ Ξ⁻ proceeded. During tagging, we recorded the Ξ⁻ signal in the silicon-strip detectors (SSD) to reconstruct the Ξ⁻ tracks in three dimensions. The stacked emulsion sheets were composed of 11 thick sheets sandwiched between 2 thin sheets, and equipped in the midst of 2 sets of SSD. All emulsion stacks were irradiated with the beam at J-PARC for 2 months. Table 1 summarises the outlines of E07.
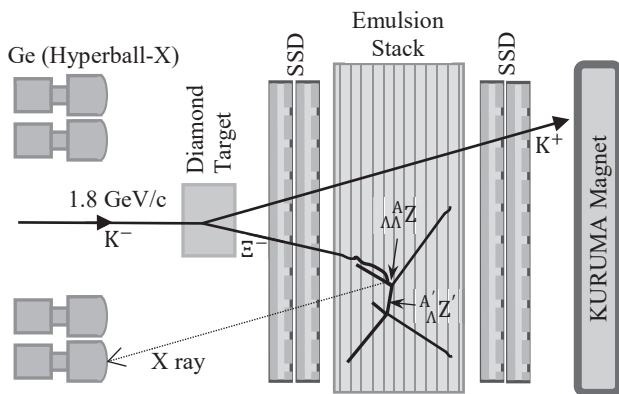

Fig 1. Experimental setup of the E07 experiment.

Table 1 Experimental condition in J-PARC E07

Beam line	K1.8
K⁻ beam quality [%]	80-85
K⁻ beam momentum	1.80 GeV/c
Expected numbers of Ξ⁻ stop	~10^4
Ξ⁻ tracking detector	SSD

Next, we conducted the photographic-development process to the irradiated sheets to amplify latent images along the path of charged particles to silver grains visible with a microscope. We used an amidol [12] developer. For the thin sheets, the temperature was kept on 10 °C in the process from presoak through fixing. For the thick sheets, we maintained all solutions in the process at 5 °C except the hot developer on 20 °C applied just after a cold (5 °C) developer. After washing of processed sheets, we soaked them into the solution with 10% glycerin to soften the dried sheets. It was taken for 8 months to develop all sheets.

After the photographic development, we searched for the Ξ⁻ tracks at the top emulsion sheet in the module and followed those tracks to downstream direction sheet by sheet using the automated microscope scanning system [13]. When we arrived at the stopping point of the Ξ⁻, we carefully observed the topology of the tracks with an optical microscope. A topology of three vertices of the tracks is a good evidence for the formation and decay of DH.

By following of Ξ⁻ tracks for 2 years, 33 DH events were detected, and some of these events, such as the MINO [8] and IBUKI [9] events, have been analysed and reported. Here, the newly detected D001 event is introduced as a new analysis of DLH. Our analysis consists of measuring the mass of the DH. To achieve this, the production and decay processes of DH were reconstructed by energy and momentum conservation obtained from the ranges and emission angles of daughter particles.

In DLH, the values of $B_{\Lambda\Lambda}$ and $\Delta B_{\Lambda\Lambda}$ are obtained from the mass as follows:

$$B_{\Lambda\Lambda}(_{\Lambda\Lambda}^{A}Z) = M(^{A-2}Z) + 2M(\Lambda) - M(_{\Lambda\Lambda}^{A}Z), \tag{1}$$

$$\Delta B_{\Lambda\Lambda}(_{\Lambda\Lambda}^{A}Z) = B_{\Lambda\Lambda}(_{\Lambda\Lambda}^{A}Z) - B_{\Lambda}(_{\Lambda}^{A-1}Z), \tag{2}$$

where Z, A, and *M* are the charge, atomic mass number, and mass, respectively. B_{Λ} is the Λ-binding energy of a single hypernucleus of $_{\Lambda}^{A-1}Z$.

The track ranges were measured via image processing on a series of several hundred micrographs taken with an objective lens 100 times in a moving lens barrel with changing a focus depth of 0.1 μm interval. The pixel size of the image corresponds to 0.143 μm on the projected image. The kinetic energy of a charged particle stopping in the emulsion layer can be obtained by summing the segmented ranges using the following range energy relation[14]:

$$R = \frac{m}{z^2} \cdot \lambda(\beta) + m\, Z^{2/3} \cdot C_Z(\beta/Z), \tag{3}$$

Where R and m are the range and the mass ratio of particle forming the track to proton mass. $\lambda(\beta)$ is the range of a proton at a velocity of βc, and C_Z is an empirical function that compensates an extension of the range of positive-charged particles caused by absorptions of electrons.

Because the thickness of the sheet was reduced via the photographic development process, the range-energy relation must be calibrated to obtain the original track ranges before shrinking. For this process, nearly 140 tracks of α-particle in the emulsion sheet, in which the D001 event was detected, were used to obtain the shrinkage factor (*SF*). The α-particles from the decay of ^{212}Po, which originated from natural isotopes of the Thorium series in the emulsion included as impurities, have a monochromatic energy of 8.784 MeV. The range of charged particles also depends upon the emulsion den-
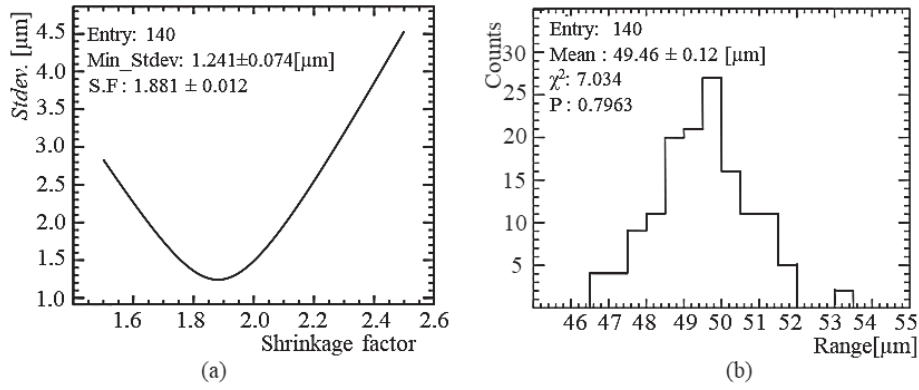
Fig 2. (a) Error of the α-range distribution as a function of *SF*. (b) Distribution of α range for the assigned *SF* of 1.881 ± 0.012.

sity. Since our emulsion has a different density from that of the standard emulsion (Ilford G5), the following equation (4) was applied to correct the range [6].

$$\frac{\lambda_s}{\lambda} = \frac{rd-1}{rd_s-1} + r\frac{(d_s-d)}{rd_s-1} \cdot \frac{\lambda_s}{\lambda_w} \tag{4}$$

Here, λ_s and λ_w are the ranges of proton tracks in the Ilford G5 emulsion and water, respectively [15], and d and d_s are the densities of our emulsion and that of Ilford G5 (3.815 g/cm³), respectively. The factor r ($= \Delta V/\Delta W$ [cm³/g]) is the ratio of the increase of emulsion volume to the mass of water absorbed in the dried emulsion sheet. The *SF* value was used as the variable in the range calculation to obtain the standard deviation error (*Stdev.*) of the range distribution. The *SF* was assigned so as to give the smallest *Stdev.* as shown in Fig 2 (a). The mean range (*R*) in the sheet before development was recalculated with the assigned *SF* by the distribution as presented in Fig 2 (b). The *SF* and *R* value of this region were 1.881 ± 0.012 and 49.46 ± 0.12 μm, respectively. Finally, the emulsion density was determined to be 3.635 ± 0.014 g/cm³ with the use of the equation (4).

We analyzed the D001 event, and Figure 3 shows the results as a superimposed image and a schematic drawing. Two charged particles (tracks #1 and #3) were emitted from the Ξ⁻ particle at the stopping point A, and track #1 decayed into two charged particles (tracks #2 and #4) at the point B. The endpoint C of track #2 showed the tracks of two charged particles (tracks #5 and #6). Table 2 lists the ranges and angles of the tracks.

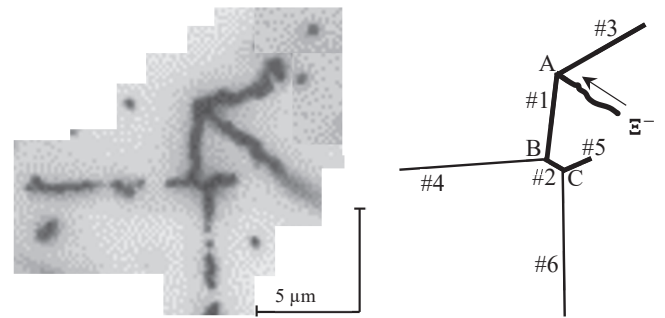The kinematic analysis described above was applied to D001. We

Fig 3. Superimposed image (left) and schematic drawing of the D001 event (right).

checked the kinematic consistency in all possible combinations of the process for the production and decay of DH. In this study, the medium-heavy nuclei of ¹²C, ¹⁴N or ¹⁶O in the emulsion were examined for at-rest capture of a Ξ⁻ particle [4][10]. The possibility of a π⁻ particle for tracks #4 and #6 was rejected because they did not show the topology of π⁻ stopping, such as the emission of auger electrons and/or nuclear fragments. According to the topologies of vertices A, B and C, at least one neutral particle will be emitted.

Table 3 lists the possible production modes. The nomination criterion was that the value of ($\Delta B_{\Lambda\Lambda} - B_{\Xi^-}$) was between -5 and 5 MeV within three standard deviations (3σ). In the case of atomic 3*D* capture of Ξ⁻ particles by ¹²C, ¹⁴N or ¹⁶O, the B_{Ξ^-} values are 0.1 - 0.2 MeV, which is negligibly small with respect to 5 MeV. In the previous E373, $\Delta B_{\Lambda\Lambda}$ has a maximal value of 2 MeV. Thus, we set the

Table 2 Ranges and angles of the tracks in D001 event.

Track	R [μm]	θ [°]	φ [°]	Comment
#1	4.1 ± 0.3	53.6 ± 3.6	82.7 ± 2.8	Double-Λ hypernucleus
#2	1.1 ± 0.2	33.7 ± 15.5	153.3 ± 20.2	Single-Λ hypernucleus
#3	5.5 ± 0.4	140.3 ± 2.1	188.4 ± 2.7	
#4	5728.6 ± 5.9	108.9 ± 2.4	2.2 ± 2.0	
#5	1.8 ± 0.5	50.6 ± 6.7	187.4 ± 9.1	
#6	1762.6 ± 2.6	55.1 ± 1.9	91.5 ± 1.6	

Table 3 Possible production modes at point A.

No.	Ξ⁻ captured		#1	#3		$B_{\Lambda\Lambda}-B_{\Xi^-}$[MeV]	$\Delta B_{\Lambda\Lambda} - B_{\Xi^-}$[MeV]
1.	Ξ⁻ + ¹²C	→	$^{8}_{\Lambda\Lambda}$Li	⁴He	n	17.50 ± 1.46	6.34 ± 1.46
2.	Ξ⁻ + ¹⁴N	→	$^{10}_{\Lambda\Lambda}$Be	⁴He	n	15.05 ± 2.78	1.63 ± 2.78

Table 4 Possible decay modes at point B.

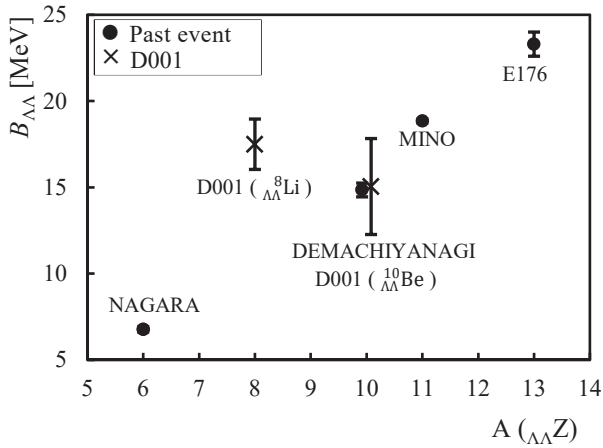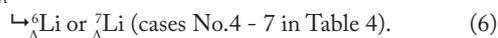| No.	DLH (#1)		#2	#4		$B_{\Lambda\Lambda}$ [MeV]	$\Delta B_{\Lambda\Lambda}$ [MeV]
1.	$_{\Lambda\Lambda}^{8}$Li	→	$_{\Lambda}^{4}$He	p	3n	<106.68 ± 0.90	<95.52 ± 0.90
2.	$_{\Lambda\Lambda}^{8}$Li	→	$_{\Lambda}^{4}$He	d	2n	<62.21 ± 2.53	<51.05 ± 2.53
3.	$_{\Lambda\Lambda}^{8}$Li	→	$_{\Lambda}^{5}$He	p	2n	<123.14 ± 1.36	<111.98 ± 1.36
4.	$_{\Lambda\Lambda}^{10}$Be	→	$_{\Lambda}^{6}$Li	p	3n	<104.29 ± 1.27	<90.64 ± 1.27
5.	$_{\Lambda\Lambda}^{10}$Be	→	$_{\Lambda}^{6}$Li	d	2n	<62.17 ± 3.42	<48.52 ± 3.42
6.	$_{\Lambda\Lambda}^{10}$Be	→	$_{\Lambda}^{7}$Li	p	2n	<106.91 ± 1.93	<93.26 ± 1.93
7.	$_{\Lambda\Lambda}^{10}$Be	→	$_{\Lambda}^{7}$Li	d	n	31.98 ± 6.65	18.33 ± 6.65

Fig 4. The $B_{\Lambda\Lambda}$ graph of observed DLH. The dots (●) and crosses (×) are obtained by the previous events and this event, respectively. With the exception of NAGARA, the past events show the most likely cases.

upper limit of the criterion to 5 MeV, and do not exclude repulsive cases as a lower limit of -5 MeV. By this criterion, multiple-neutron emissions were rejected.

At the vertex B in Fig 3, the decay modes with one-neutron emission are nominated, if the value of $\Delta B_{\Lambda\Lambda}$ are to be between -5 and 5 MeV within 3σ. For the modes of multiple-neutron emission, we don't set the upper limit (5 MeV) of $\Delta B_{\Lambda\Lambda}$, because we can only obtain the minimum momentum of neutrons due to the impossibility of specifying their emission direction. There are 42 possible cases of $_{\Lambda\Lambda}$Li, $_{\Lambda\Lambda}$Be, $_{\Lambda\Lambda}$B, and $_{\Lambda\Lambda}$C decays at the vertex B. Based on the production modes in Table 3, the possible decay modes are restricted to $_{\Lambda\Lambda}^{8}$Li and $_{\Lambda\Lambda}^{10}$Be, and listed in Table 4.

Figure 4 presents a comparison of the $B_{\Lambda\Lambda}$ to the mass number A ($_{\Lambda\Lambda}$Z) for the candidates of D001 according to the possible production process in Table 3 and the ones taken from the past analyses [4) 5) 8)]. Because the plotting point for the case No.1 in Table 3 is far from the line of $B_{\Lambda\Lambda}$ to A ($_{\Lambda\Lambda}$Z), $_{\Lambda\Lambda}^{10}$Be as the case No.2 seems most likely to the nuclide in this D001 event.

Therefore, D001 can be interpreted as follows:

$$\Xi^- + {}^{14}N \rightarrow {}_{\Lambda\Lambda}^{10}Be + {}^4He + n, \tag{5}$$

$$\hookrightarrow {}_{\Lambda}^{6}Li \text{ or } {}_{\Lambda}^{7}Li \text{ (cases No.4 - 7 in Table 4).} \tag{6}$$

where, $_{\Lambda}^{6}$Li or $_{\Lambda}^{7}$Li, in the equation (6) was understood as a decay with multiple-neutron emissions.

Taking into account the B_{Ξ^-} value of 0.17 MeV for the atomic 3D orbit of the ^{14}N + Ξ^- system [16)], as well as the B_{Λ} of 6.71 ± 0.04 MeV of $_{\Lambda}^{9}$Be [17)] at $_{\Lambda\Lambda}^{10}$Be production, we find that the values of $B_{\Lambda\Lambda}$ and $\Delta B_{\Lambda\Lambda}$ are 15.22 ± 2.78 MeV and 1.80 ± 2.78 MeV, respectively. Although

the error is as large as one order of magnitude for the data from the NAGARA and MINO event due to the neutron emission, the Λ-Λ interaction strength, $\Delta B_{\Lambda\Lambda}$, agrees with these two events.

In the E07 experiment, 33 double-hypernuclear events were detected by following the Ξ^- tracks for 2 years, meanwhile a new scanning method (called the overall-scanning method [18)]) will be applied to search for DH, and it is expected to detect nearly 1,000 DH events within a few years.

Acknowledgement

References

1) M. Danysz, K. Garbowska, J.Pniewski, T. Pniewski and J. Zakrzewski, Nucl. Phys., **49**, 121 (1963).

2) S. Aoki, K. Imai, M. Nakamura, K. Nakazawa, N. Yasuda, and 54 others, Nucl. Phys. A, **644,** 365 (1998).

3) H. Takahashi, A. Ichikawa, K. Imai, K. Nakazawa, and 63 others, Phys. Rev. Lett. **87**, 212502 (2001).

4) S. Aoki, K. Imai, K. Nakazawa, H. Takahashi, C. S. Yoon, and 55 others, Nucl. Phys. A, **828**, 191 (2009).

5) J. K. Ahn, A. Ichikawa, K. Imai, K. Nakazawa, H. Takahashi, and 73 others, Phys. Rev. C, **88**, 014003 (2013).

6) K. Nakazawa, K. Imai, S. Kinbara, M. K. Soe, H. Takahashi, K. T. Tint, J. Yoshida, and 17 others, Prog. Theor. Exp. Phys., **2015**, 033D02 (2015).

7) E. Hiyama and K. Nakazawa, Annu. Rev. Nucl. Part. Sci., **68**, 131 (2018).

8) H. Ekawa, M. Fujita, S. H. Hayakawa, A. Kasagi, K. Nakazawa, A.N.L. Nyaw, J. Yoshida, M. Yoshimoto, and 95 others, Prog. Theor. Exp. Phys., **2019**, 021D02 (2019).

9) S. H. Hayakawa, H. Ekawa, M. Fujita, A. Kasagi, K. Nakazawa, A.N.L. Nyaw, J. Yoshida, M. Yoshimoto, and 89 others, (arxiv.org/abs/2010.14317).

10) A. M. M. Theint, S. Kinbara, K. Nakazawa, J. Yoshida, M. Yoshimoto, and 5 others, Prog. Theor. Exp. Phys., **2019**, 021D01 (2019).

11) T. Nakamura, M. Nakamura, and 35 others, Nucl, Instrum, Meth. Phys. Res. A, **556**, 80, (2006).

12) TOKYO CHEMICAL INDUSTRY CO., LTD., https://www.tcichemicals.com/JP/en/p/D0080.

13) M. K. Soe, R. Goto, A. Mishina, Y. Nakanisi, D. Nakashima, J. Yoshida and K. Nakazawa, Nucl. Instrum. Meth. Phys. Res. A, **848**, 66 (2017).

14) H. H. Heckman, B. L. Perkins, W.G Simon, F. M. Smith and W. H. Barkas, Phys. Rev., **117**, 544, (1960).

15) W. H. Barkas, P. H. Parrett, P. Cüer and H. H. Heckman, Nuovo Cimento, **8**, 185, (1958).

16) M. Yamaguchi, K. Tominaga, Y. Yamamoto and T. Ueda, Prog. Theor. Phys., **105**, 627, (2001).

17) D. H. Davis, Contemp. Phys. **27**, 91 (1986).

18) J. Yoshida, S. Kinbara, A. Mishina, K. Nakazawa, M. K. Soe, A. M. M. Theint and K. T. Tint, Nucl. Instrum. Meth. Phys. Res. A, **847**, 86 (2017).